This is a peer-reviewed version that has been accepted (pending final editions) for publication in Terra Nova on 24/07/2023

Emplacement and associated sedimentary record of the Jurassic submarine salt allochthon of the Wurzeralm (Eastern Alps, Austria)

Maditha Kurz[1], Oscar Fernandez[1], Lino Eggerth[1], Bernhard Grasemann[1], Philipp Strauss[2]

[1] Dept. of Geology, University of Vienna, Josef-Holaubek-Platz 2 (UZA II), 1090 Vienna, Austria

[2] OMV, Trabrennstrasse 6-8, 1020 Vienna, Austria

Corresponding author:

Oscar Fernandez
@itsoscarsfault
oscar.fernandez.bellon@univie.ac.at
+43 1 4277 53609
Dept. of Geology
UZA2 B446A
Josef-Holaubek-Platz 2
1090 Wien, AUSTRIA
ORCID: 0000-0003-1584-2684

Abstract

A fossil salt sheet emplaced in the Jurassic in submarine conditions is described in the Eastern Alps of Austria, providing unique insights into the emplacement of similar submarine structures and their potential control on depositional systems. The salt sheet is a plug-fed extrusion emplaced due to squeezing of a salt diapir under compression. The preserved mylonitic shear fabric in the evaporites indicates radial, south-directed emplacement of the salt sheet. Tectono-sedimentary relationships record the evolution of the salt structure, from initial diapiric growth, to salt sheet extrusion and posterior collapse. Syn-extrusion sediments record the variable bathymetry of the extruding salt sheet, with reefal carbonates building up on the crestal bulge while their deeper water equivalents accumulated on the extruding salt lobe. This is the first description of a salt allochthon still linked to its source diapir in the Eastern Alps.

Introduction

Allochthonous salt bodies are common features of salt basins worldwide and have been abundantly documented in both convergent and passive margin settings (Hudec and Jackson, 2006; Rowan, 2017). The mechanism of emplacement of these bodies has been studied in detail in the Zagros *namakiers*, emplaced subaerially (Schleder and Urai, 2007; Mansouri et al., 2019; Závada et al., 2021). In other contexts, outcrop conditions (weathering, vegetation), tectonic overprint or inaccessibility (as in submarine examples) make similar analysis impossible.

In this paper we present a uniquely well-preserved example of a plug-fed extrusion (*sensu* Hudec and Jackson, 2006) emplaced in a submarine setting in the Late Jurassic. The allochthonous salt sheet is located in the Northern Calcareous Alps (Eastern Alps, Austria), and has been mostly preserved in its original geometry, in spite of post-extrusion Alpine deformation. The extruded evaporite body (made up at present mostly of gypsum) excellently preserves original extrusion shear fabrics and syn-emplacement roof sediments. This paper summarizes the available field evidence to provide a kinematic and tectono-sedimentary model for salt sheet extrusion in submarine settings.

Geological Setting

The Northern Calcareous Alps (NCA) are a set of imbricate thrust sheets of Upper Permian to Eocene strata mostly detached from their Variscan basement (Wagreich and Faupl, 1994; Linzer et al., 1995; Schmid et al., 2004). The NCA Upper Permian to Middle Jurassic succession was deposited on Adria, a continental block forming the northern passive margin of the Neo-Tethys (Mandl, 2000; Schmid et al., 2008). From Middle to Late Jurassic, Adria rifted and separated from Europe forming the Alpine Tethys (Mandl, 2000; Schmid et al., 2008). An early phase of Alpine orogenesis in the Late Jurassic caused initial inversion of the margin and shortening in the NCA (Frank and Schlager, 2006; Gawlick and Missoni, 2019; Fernandez et al., in review). From Early Cretaceous to Paleogene times the NCA were thrust over the Alpine Tethys and European continental margin (Linzer et al., 1995; Stüwe and Schuster, 2010).

Mandl (2000) provides an overview of the NCA stratigraphy, summarized here (Fig. 1b). An initial Upper Permian red bed succession deposited during rifting is overlain by the Permo-Triassic Haselgebirge Fm, a thick sequence of evaporites and shales (Leitner et al., 2017). These units are followed by late rift Lower Triassic epi-continental clastics (Werfen Fm) and Middle Triassic shallow water carbonates (Gutenstein Fm). Thermal subsidence and salt-evacuation during the Middle to Late Triassic provided accommodation space for the deposition of a 2 to 3 km thick sequence of shallow platform carbonates (Wetterstein and Dachstein Limestones) that record syn-depositional diapir growth in the form of rapid thickness changes and folding (Fig. 2) (cf. Fernandez et al., 2021; Strauss et al., 2021). The Reifling Fm and the Hallstatt Limestone (absent in the study area) are their deep water equivalents.

Continued subsidence in combination with reduced carbonate productivity during the Early Jurassic led to the drowning of platforms and the accumulation of condensed deep water

red crinoidal limestone above submarine swells (Adnet Fm) and a marly turbidite succession in intervening basins (Allgäu Fm). Middle Jurassic is also condensed stratigraphy an represented by the Mn-nodule rich, red Klaus Fm, and/or the Ruhpolding Fm radiolarites and siliceous limestones. A major change occurred in the Upper Jurassic, with the deposition of the shallow water reefal Plassen Limestone and its deeper water marly limestone equivalent (Oberalm Fm). The Upper Jurassic is also characterized by the presence of localized pockets of breccias (Rofan Breccia, *sensu* Ottner, 1990).

The youngest deposits in the area are syn-orogenic clastics of the Gosau Group (Wagreich and Decker, 2001).

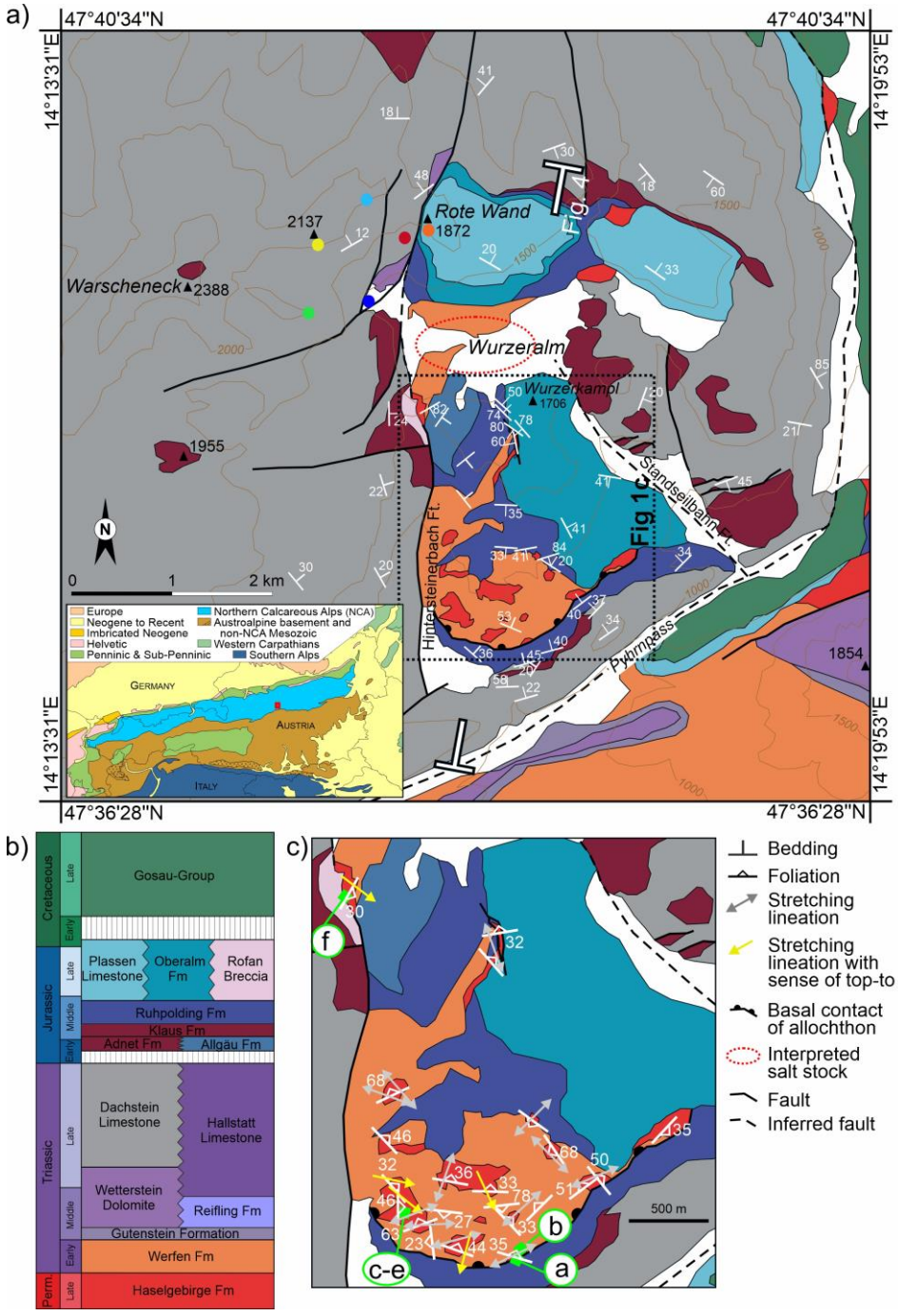

Fig. 1 a) Detailed geological map of the Wurzeralm and surrounding area (after Ottner, 1990; Moser and Pavlik, 2014; Kurz, 2022; and mapping by the authors) with bedding dip measurements. The color legend follows the scheme in (b). The inset shows the location of the study area within the Eastern Alps (red box). The colored dots in the area of the Warscheneck-Rote Wand are points shown also in Figure 2 for location reference. The location of (c) and of the profile in Figure 4 are shown. b) Simplified stratigraphic chart of the area roughly scaled for the relative thickness of units in the area. c) Detail of the Wurzeralm salt sheet, south of the inferred salt stock feeder, with foliation (and their dip magnitude) and stretching lineations measured in Haselgebirge Fm gypsum. Lineations that are accompanied by shear sense indicators are shown as unidirectional arrows indicating "top-to-the" direction. The location of the photographs in Figure 3 is indicated by labels a-f.

The Wurzeralm salt sheet

The Wurzeralm salt sheet is located on the trailing (southernmost) edge of the preserved central NCA thrust sheets. The Wurzeralm diapir and salt sheet outcrop define a roughly N-S rectangular area characterized by a somewhat patchy arrangement of Jurassic units and Haselgebrige and Werfen Fms (Fig. 1a), completely surrounded by the Dachstein Limestone and Adnet and Klaus Fms (Fig. 1a).

West of the Wurzeralm, the Dachstein Limestone thins against the diapir, indicating syn-depositional diapir growth (Fig. 2).

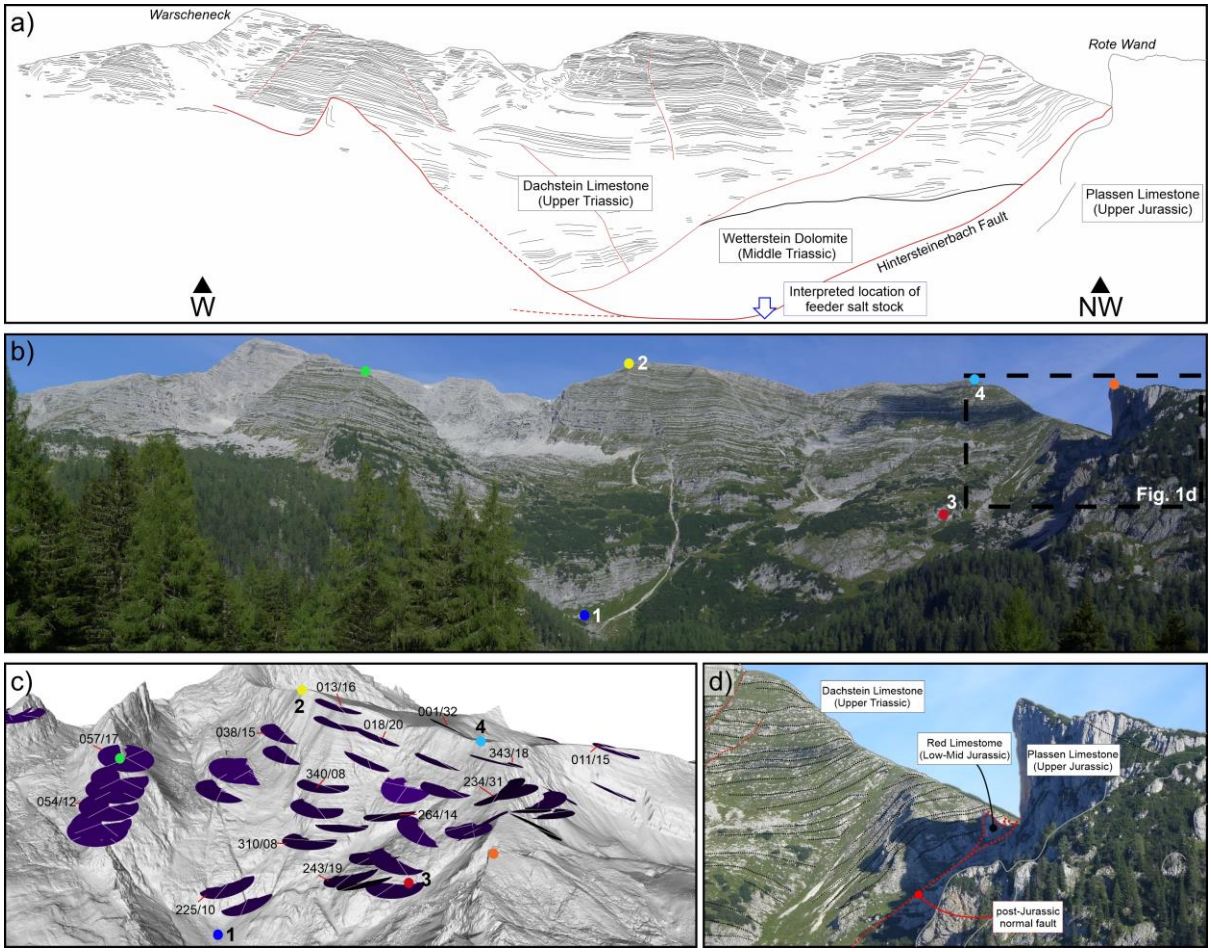

Fig. 2 a,b) Panorama looking west of the Wurzeralm, and line drawing showing a thinning of the Dachstein Limestone towards the Wurzeralm diapir. The Plassen Limestone of the Rote Wand sits above the collapsed Wurzeralm diapir. c) Oblique view of a Lidar digital terrain model of the area in the panorama in (a) (digital terrain model data obtained from Land Oberösterreich - data.ooe.gv.at, under CC-BY-4.0 license). Blue disks represent bedding dip and show progressive rotation of the beds, from the bottom to the top of the Dachstein Limestone. Colored dots represent reference points in (b) (shown also in Figure 1a). The stratigraphic thickness of the Dachstein Limestone reduces from 800 m between dots labelled 1 and 2, to 500 m between dots labelled 3 and 4. d) Detail from the panorama in (a) showing a small-scale syncline developed in the Dachstein Limestone in the proximity to its contact with the diapir.

Along its southern outcrop edge, the Haselgebirge Fm of the Wurzeralm rests directly on the Ruhpolding Fm. The contact between both units is masked by vegetation in outcrop (Fig. 3a, Supplemental information 1), but geological mapping shows the surface dips under the Haselgebirge Fm, parallel to bedding of the underlying Ruhpolding Fm (Fig. 1a, Supplemental information 2). Whereas the Ruhpolding Fm is undeformed and concordant with the underlying stratigraphy, the Haselgebirge presents a penetrative mylonitic fabric indicating south-directed emplacement (Fig. 3b). Isolated levels of Dachstein Limestone sedimentary breccias have been found within the Ruhpolding Fm under the salt sheet (Fig. 3a).

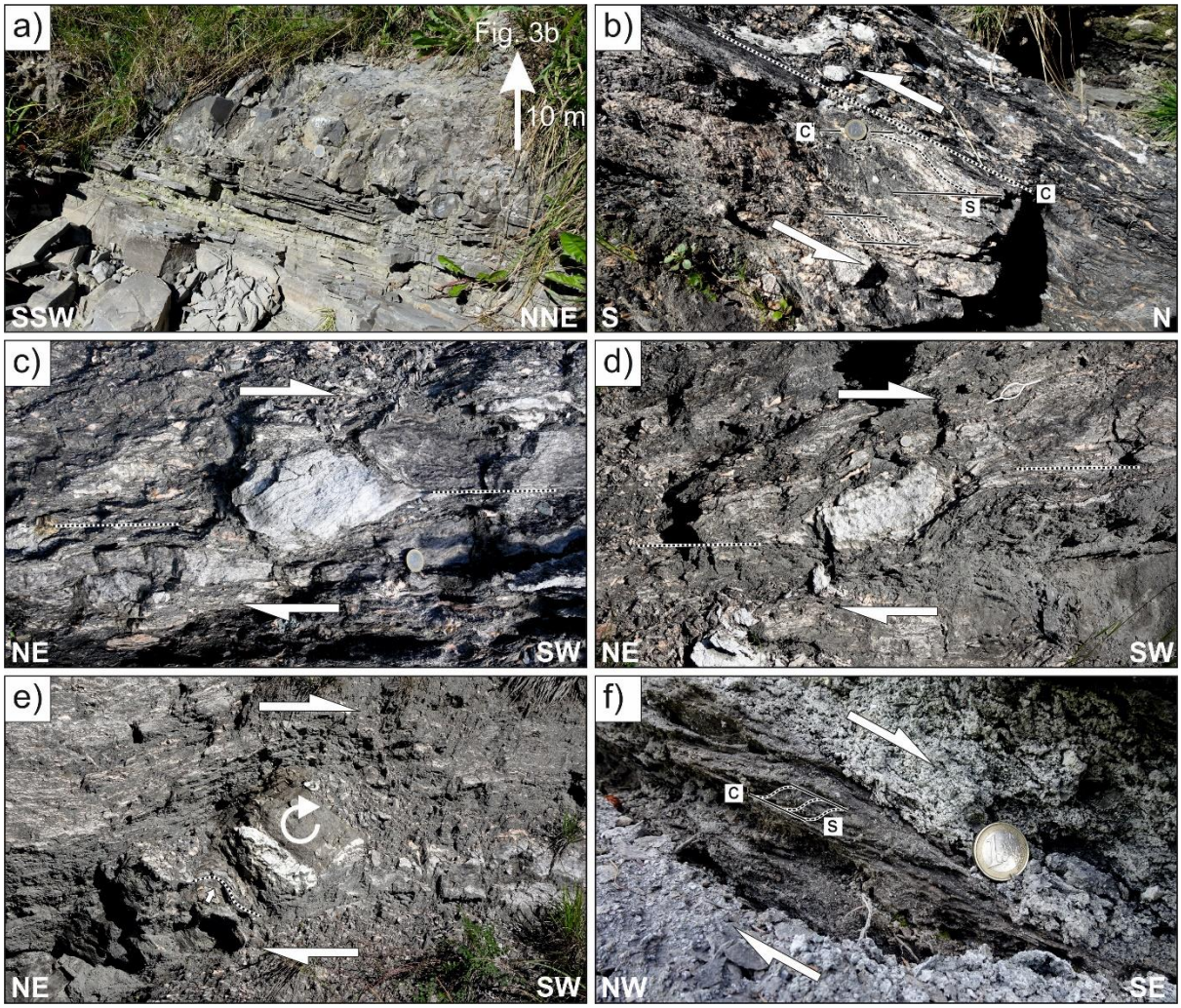

Fig. 3 a) Conglomerate layer with up to 15 cm large limestone components in the otherwise planar cm-bedded siliceous limestone of the Ruhpolding Fm. This outcrop (UTM33 446336E, 5274432N) is 6 meters stratigraphically below the Haselgebirge (Fig. 3b). b) Mylonitic Haselgebirge (UTM33 446333E, 5274444N) with scc' fabric indicating top-to-the south shear sense (c-plane 350/38, stretching lineation on c-plane 005/36). c and d) Sigmoidal shaped anhydrite components stabilized with long axes inclined against the shear direction. Note, the stair stepping of the foliation in the Haselgebirge indicating top-to-the SW shear sense (UTM 33 445676E, 5274675N). e) Rolling structure of an angular sandstone clast coupled with the foliation in the Haselgebirge (UTM33 445690E, 5274658N). The clear embayment of the foliation in the Haselgebirge (grey arrow) suggests a co-shearing rotation of the clast

indicating top-to-the SW shear sense. f) Sigmoidal secondary foliation s (305/08) in the Haselgebirge dips against the top-to-the SE shear sense on the c-planes (114/33). The stretching lineation (126/32) on the c-planes is roughly perpendicular to the intersection of the s- and c-planes (UTM33 445288E, 5276731N). Location of all figures is shown in Figure 1c.

The Haselgebirge Fm in the area is characterized by mylonitic fabric similar to that observed along its southern margin (3c-f). Stretching lineations and shear sense indicators in the gypsum consistently show top-to-the-south shearing (ranging between southwest and southeast) (Fig. 1c). Along the southern outcrop border, the stretching direction is somewhat variable, recording non-plane-strain finite deformation (Fig. 1c).

The Haselgebirge Fm is overlain mostly by the Werfen Fm and locally directly by the Allgäu and Ruhpolding Fms (Fig. 1b). The Ruhpolding Fm is intensely folded, with fold axes trending in two perpendicular directions. One trends NE-SW (azimuth 020-070) and the other NW-SE (azimuth 300-320). The NE-SW fold trend is not observed in younger lithologies, nor does it coincide with the local shearing direction in the Haselgebirge Fm, and is therefore potentially related to soft-sediment deformation above the Wurzeralm diapir during deposition (Supplemental Information 3). The NW-SE trend in turn, is parallel to thrusts and folds involving the Oberalm and Haselgebirge Fms that potentially conditioned fabric development in the Haselgebrige Fm locally (Supplemental Information 3).

The Wurzeralm salt sheet is capped by the Plassen and Oberalm Fms. The reefal Plassen Limestone in the north transitions to the deeper water Oberalm Fm to the south. At present, the Plassen Limestone of the Wurzeralm lies at an elevation equivalent to that of the Dachstein Fm west of the Wurzeralm diapir due to activity of a post-Jurassic eastward dipping normal fault (Fig. 2d).

Along the western margin of the diapir, Rofan Breccia deposited along the edge of the evaporite body contain reworked limestone fragments of the Dachstein, Allgäu and Oberalm Fms, dark shale fragments that likely originate from the Haselgebirge Fm, and isolated clasts of Hallstatt Limestone (Ottner, 1990).

Discussion

The structure and outcrop distribution of the study area is interpreted to show the relict structure of a southward-directed plug-fed extrusion (Fig. 4). Extrusion of the Haselgebirge Fm onto the seafloor above Middle Jurassic sediments occurred during the Late Jurassic (Fig. 5) and was driven by shortening of the diapiric salt stock. Based on the stretching lineations (Fig. 1c) we interpret a dominantly southeast- to southwestward emplacement. Stretching perpendicular to the south-directed flow along the southern front of the allochthon and at a location below the Ruhpolding Fm (Fig. 1c) is non-directional and likely due to transverse (circumferential) extension in the shallower portions of the allochthon (analogue to that modelled for axisymmetrical extrusive flow; Buisson and Merle, 2004; Zavada et al., 2009).

We interpret that the salt stock that fed the salt sheet is located south of the Rote Wand (Figs. 1a, 2a, 4) given that: 1) here the Werfen Fm outcrops lie deeper than the Middle Jurassic of the Rote Wand (i.e., in non-allochthonous position) (Fig. 2a); 2) this location is north of the northermost south-directed shear indicator (Fig. 1c); and 3) this area and the

Rote Wand were the shallowest during the Late Jurassic (shallowest water facies; Fig. 5) which could be explained by crestal doming above the salt stock during allochthony (e.g., Dooley et al., 2015) and upward tilting of the northern diapir flank (Fig. 5). Uplift of this flank led to erosion of the Lower to Middle Jurassic under the Rote Wand (Fig. 1a). The location of the southern wall of the salt stock is expected to be north of the northermost south-directed shear indicator (Fig. 1c). The width of the salt stock in Figure 4 is taken from the analogous Hallstatt diapir (Fernandez et al., 2021).

The present-day structure suggests that the allochthonous salt sheet was at least 500 m thick (Fig. 4), a magnitude compatible with dynamic topographies documented in plug fed extrusions (e.g., Dooley et al., 2015). The present-day elongate asymmetric shape of the salt sheet and the absence of Upper Jurassic deposits beyond the faults we name here Hintersteinerbach and Standseilbahn faults (Fig. 1a), suggests these faults bounded the salt sheet during emplacement. These faults are interpreted to cut across the entire Triassic stratigraphy, as indicated by the fact that a splay of the Hintersteinerbach juxtaposes the Dachstein Fm against the Wetterstein Fm (Fig. 2a), and the panel of Triassic platform they bound may have been tilted down northwards during shortening (Fig. 5), guiding the emplacement of the salt sheet. The northern extension of the Hintersteinerbach fault was later activate in extension (possibly during the Late Cretaceous, similar to structures documented further west by Fernandez et al., 2022), dropping the Jurassic Plassen Limestone down to the same elevation as the Dachstein Limestone (Fig. 2a,d).

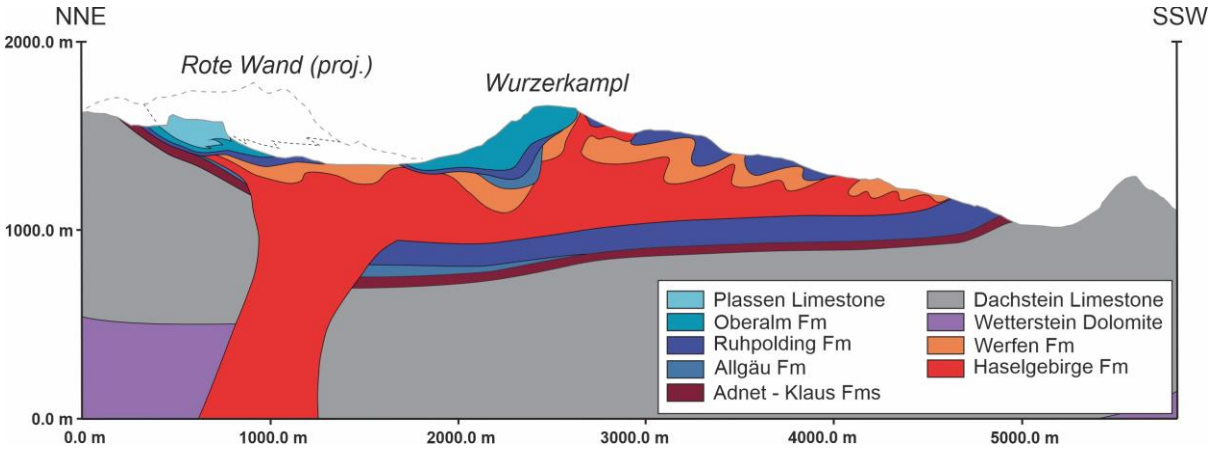

Fig. 4 Structural cross-section across the Wurzeralm salt allochthon. Structure at depth is inferred, including the regional thickness of the Dachstein Limestone derived from constraints beyond the study area.

The link between deformation of the evaporites and that of the overlying units is not univocal. As discussed above, NE-SW trending folds in the Ruhpolding Fm likely relate to syn-sedimentary deformation atop the diapir (Supplemental Information 3). Diapir-related instability potentially also affected surrounding areas, as recorded by the presence of breccias in the sub-allochthon Ruhpolding Fm (Fig. 3a). Posteriorly, during emplacement, roof units were likely passively dismembered (e.g., Dooley et al., 2015), and partly eroded and accumulated in the Rofan Breccia bodies above and ahead of the open-toe allochthon front. Notwithstanding, NW-SE trending folds and thrusts in the Ruhpolding and Oberalm Fm also involved deformation with the Haselgebirge Fm (Supplemental Information 3). These

structures are tentatively related to constriction of the salt sheet between the Hintersteinerbach and Standseilbahn faults (Fig. 1a).

Although the Wurzeralm structure has previously been explained as the result of gravitational northward sliding (Lein, 1987a; Ottner, 1990; Tollmann, 1987), the top-to-the-south shear in the gypsum of the Haselgebirge Fm (Fig. 3) rules out a south-derived origin for the Wurzeralm salt (either by sliding or by thrusting). Southward emplacement of the salt sheet can be accounted for by an episode of Jurassic compression-driven allochthony (Fig. 5). The mylonitic fabric likely developed through pressure solution-precipitation creep (e.g., Závada et al., 2021) and required rates of deformation that are more compatible with gradual allochthony than with near instantaneous gravitational sliding. Furthermore, a similar history of Triassic diapir growth and Jurassic shortening, as opposed emplacement of the Haselgebirge evaporites by gravitational sliding, has been documented by Fernandez et al. (2021) in the Hallstatt diapir, some 50 km to the west. The Wurzeralm is in line with a growing body of examples recently highlighting the relevance of salt tectonics in the NCA Granado et al. (2019) and Strauss et al. (2021).

Schorn and Neubauer (2011) also documented mylonitic fabric in Haselgebirge Fm anhydrite in the Moosegg body (some 100 km to the west), but interpreted it as necessarily resulting from thrusting. Our observations and those of Zavada et al. (2021) indicate that mylonitic fabric in anhydrite can develop at shallow levels, making it possible to propose a possible alternative origin for the Moosegg body as an allochthon. The capping of the Moosegg body by Lower Cretaceous clastics, and the presence of fragments of Haselgebirge within the Lower Cretaceous sediments surrounding it (Schorn and Neubauer, 2011) could be explained by surface exposure of the Haselgebirge Fm during allochthony. An equivalent situation is that of the Bad Ischl salt accumulation, which rests on Lower Cretaceous sediments (Mandl et al., 2012). MORB-affinity igneous rocks found within both of these bodies (Vozarova et al., 1999; Schorn et al., 2013), not expected in diapirs soled above continental crust, are common components of Lower Cretaceous clastics (Krische et al., 2014) and might have been incorporated during emplacement.

Likewise, occurrences of Haselgebrige Fm on a Middle Jurassic seafloor documented at other locations in the NCA (e.g., Plöchinger, 1996; Suzuki and Gawlick, 2009; Mandl, 2016) might be candidates to evaluate as the possible result of salt allochthony.

The Wurzeralm also provides important insights into the Jurassic bathymetric evolution of the area. It is generally accepted that the NCA deepened during the Early to Middle Jurassic culminating during deposition of the Ruhpolding Fm (Lein, 1987b; Mandl, 2000). Uplift of the seafloor into the photic zone during the Late Jurassic was necessary for the growth of Plassen Limestone reefs. Plassen reefs occur in the NCA mostly as isolated reefs, often above Haselgebirge Fm accumulations (Tollmann, 1976, 1987). Uplift driven by doming of salt above its stock during extrusion (Fig. 5) can account for the isolated nature of reef development, with the crestal bulge being the only point to bathymetrically rise into the photic zone. For this to be possible, assuming up to 1000 m of salt-driven uplift (Dooley et al., 2015), the Ruhpolding Fm must have deposited in water not much deeper than 1000 m (compatible with the depth of other Tethyan Jurassic radiolarites; Baumgartner, 2013). In the

absence of regional uplift, sedimentation during the Late Jurassic would have focused around the developing reef, as indicated by the absence of Upper Jurassic sediments to the west and north of the Wurzeralm (Fig. 1a; Moser and Pavlik, 2014) and by their greatly reduced thickness further to the east (Tollmann, 1976).

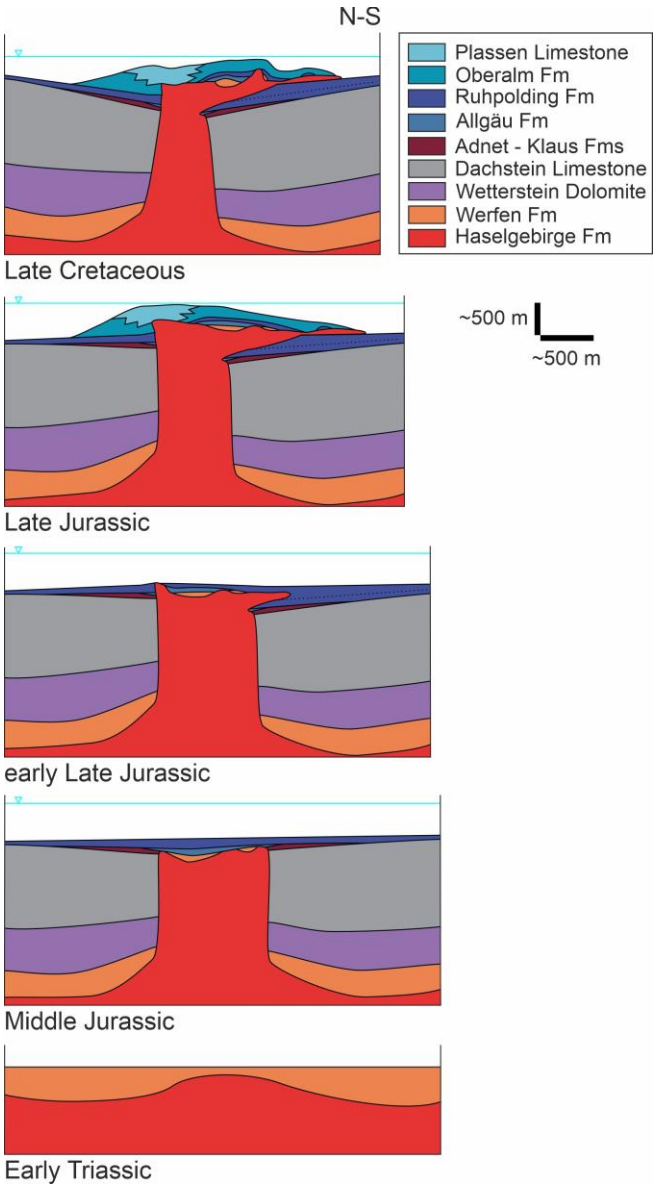

Fig. 5 Conceptual evolutionary model of the Wurzeralm salt sheet. Sketch not to scale (approximate horizontal and vertical scales provided). The Triassic evolution of the structure was dominated by passive growth of a diapir and deposition of the Wetterstein and Dachstein Fms in flanking minibasins. This was followed by a period of quiescence and partial subsidence of the diapir during Early to Middle Jurassic. During this period, condensed red limestones (Adnet/Klaus Fms) deposited on the shallower minibasins flanking the diapir and the Allgäu Fm mainly over the subsiding diapir. This whole suite was draped over by the Ruhpolding Fm. Initial shortening in Late Jurassic times led to initial allochthony, synchronous with deposition of the youngest Ruhpolding Fm. As allochthony developed fully, both flanks of the diapir were tilted; the southern one downwards and the northern one upwards. The Upper Jurassic Plassen and Oberalm Fms deposited during this phase, with the shallower Plassen reef growing preferentially above the salt stock and the tilted northern flank of the diapir. Finally, during Late Cretaceous times, the salt structure collapsed partially to its almost present-day structure.

Conclusion

Despite the magnitude of Alpine overprint in the area, the Jurassic-age Wurzeralm salt sheet presents an almost intact structure and is a striking example of a submarine-emplaced allochthonous salt body with syn-emplacement roof sedimentation. This salt sheet constitutes the first instance of a preserved diapir and its associated allochthon documented in the Eastern Alps, underscores the relevance that salt tectonics played in this area, and highlights the need of revisiting the interpretation of other salt bodies in the Eastern Alps.

Acknowledgements

The authors wish to thank P. Zavada, M.J. Dekkers and an anonymous reviewer for their insightful comments. M. Kurz was funded by the W. Schöllnberger Student Fund and Geosphere Austria (under H.-G. Krenmayr). Research by O. Fernandez and L. Eggerth is supported by the FFG and Salinen AG FFG-Bridge Project ETAPAS (FO999888049), by FWF Project POLARIS (I5399-N), and by Project SABREM, PID2020-117598GB-I00 (MCIN/ AEI /10.13039/501100011033). Academic licenses of Move software are provided by Petex Ltd.

References

Baumgartner, P.O., 2013. Mesozoic radiolarites – accumulation as a function of sea surface fertility on Tethyan margins and in ocean basins. *Sedimentology*, **60**, 292-318. doi: 10.1111/sed.12022

Dooley, T.P., Jackson, M.P.A., Hudec, M.R., 2015. Breakout of squeezed stocks: dispersal of roof fragments, source of extrusive salt and interaction with regional thrust faults. *Basin Research*, **27**, 3-25. doi: 10.1111/bre.12056

Fernandez, O., Habermüller, M. and Grasemann, B., 2021. Hooked on salt: Rethinking Alpine tectonics in Hallstatt (Eastern Alps, Austria). *Geology*, **49**, 325-329. doi: 10.1130/G47981.1

Fernandez, O., Grasemann, B. and Sanders, D., 2022. Deformation of the Dachstein Limestone in the Dachstein thrust sheet (Eastern Alps, Austria). *Austrian Journal of Earth Sciences*, **115**, 167-190. doi: 10.17738/ajes.2022.0008

Fernandez, O., Ortner, H., Sanders, D., Grasemann, B., Leitner, T., in review. Mesozoic paleogeography, structural configuration and evolution of the central Northern Calcareous Alps (Eastern Alps, Austria): Alternative scenarios and discussion. *International Journal of Earth Sciences*. Pre-print: https://doi.org/10.31223/X55M2X

Frank, W., and Schlager, W., 2006. Jurassic strike slip versus subduction in the Eastern Alps. *International Journal of Earth Sciences*, **95**, 431-450. doi: 10.1007/s00531-005-0045-7

Gawlick, H.-J. and Missoni, S., 2019. Middle-Late Jurassic sedimentary mélange formation related to ophiolite obduction in the Alpine-Carpathian-Dinaridic Mountain Range. *Gondwana Research*, **74**, 144-172.

Granado, P., Roca, E., Strauss, P., Pelz, K. and Muñoz, J.A., 2019. Structural styles in fold-and-thrust belts involving early salt structures: The Northern Calcareous Alps (Austria). *Geology*, **47**, 51-54. doi: 10.1130/G45281.1

Hudec, M. and Jackson, M., 2006. Advance of allochthonous salt sheets in passive margins and orogens. *AAPG Bulletin*, **90**, 1535-1564.

Lein, R., 1987a. Zur Verbreitung der Hallstätter Zone beiderseits des Pyhrn-Passes. *OÖ Geonachrichten*, **2**, 21-37.

Lein, R., 1987b. Evolution of the Northern Calcareous Alps during Triassic times. In: *Geodynamics of the Eastern Alps* (H. Flügel and P. Faupl, eds.) Franz Deuticke, Vienna, 85-102.

Leitner, C., Weismaier, S., Köster, M.H., Gilg, H.A, Finger, F. and Neubauer, F., 2017. Alpine halite-mudstone-polyhalite tectonites: Sedimentology and early diagenesis of evaporites in an ancient rift setting (Haselgebirge Formation, eastern Alps). *Geological Society of America Bulletin*, **129**, 1537-1553. doi:10.1130/B31747.1.

Linzer, H.-G., Ratschbacher, L. and Frisch, W., 1995. Transpressional collision structures in the upper crust: the fold-thrust belt of the Northern Calcareous Alps. *Tectonophysics*, **242**, 41-61.

Krische, O., Goričan, Š., Gawlick, H.-J., 2014. Erosion of a Jurassic ophiolitic nappe-stack as indicated by exotic components in the Lower Cretaceous Rossfeld Formation of the Northern Calcareous Alps (Austria). *Geologica Carpathica*, **65**, 3-24. doi: 10.2478/geoca-2014-0001

Kurz, M., 2022. Struktur und Entstehung eines jurassischen allochthonen Salzkörpers der "Wurzer Diapir": Neukartierung eines Teilabschnittes des Kartenblattes 98-Liezen (Nördliche Kalkalpen, Österreich). Unpubl. Master's thesis, University of Vienna, Vienna.

Mandl, G.W., 2000. The Alpine sector of the Tethyan shelf – Examples of Triassic to Jurassic sedimentation and deformation from the North Calcareous Alps. *Mitteilungen der Österrichischen Geologischen Gesellschaft*, **92**, 61-77.

Mandl, G.W., 2016. Das Kalkalpine Stockwerk auf GK50 Blatt 103 Kindberg. In: *Arbeitstagung 2015 der Geologischen Bundesanstalt Geologie der Kartenblätter GK50 ÖK 103 Kindberg und ÖK 135 Birkfeld, Mitterdorf im Mürztal 21.–25 September 2015* (R. Schuster and T. Ilickovic, eds.) Geologische Bundesanstalt, Vienna, 88-101.

Mansouri, H., Prior, D.J., Ajalloeian, R. and Elyaszadeh, R., 2019. Deformation and recrystallization mechanisms inferred from microstructures of naturally deformed rock salt from the diapiric stem and surface glaciers of a salt diapir in Southern Iran. *Journal of Structural Geology*, **121**, 10-24. doi: 10.1016/j.jsg.2019.01.005

Moser, M. and Pavlik, W., 2014. Blatt 98 Liezen 1:50.000. In: *Zusammenstellung ausgewählter Archivunterlagen der Geologischen Bundesanstalt GEOFAST 1:50.000* (Krenmayr, H.G, ed.), Verlag der Geologischen Bunesanstalt, Vienna.

Ortner, H., 2017. Geometry of growth strata in wrench-dominated transpression: 3D-model of the Upper Jurassic Trattberg rise, Northern Calcareous Alps, Austria. EGU General Assembly, 23-28 April, Vienna, Austria.

Ottner, F., 1990. Zur Geologie der Wurzer Deckenscholle und deren Rahmen im Bereich des Warschenecks (OÖ). *Mitteliungen der Gesellschaft der Geologie- und Bergbaustudenten Österreichs*, **36**, 101-145.

Plöchinger, B., 1996. Das Halleiner Salinargebiet (Salzburg) im Geotopschutz-Projekt. *Jahrbuch der Geologischen Bundesanstalt*, **139**, 497-504.

Rowan, M.G., 2017. An Overview of Allochthonous Salt Tectonics. In: *Permo-Triassic Salt Provinces of Europe, North Africa and the Atlantic Margins* (J.I. Soto, J.F. Flinch and G. Tari, eds.) Elsevier, 97-114. doi: 10.1016/B978-0-12-809417-4.00005-7

Schleder, Z. and Urai, J.L., 2007. Deformation and recrystallization mechanisms in mylonitic shear zones in naturally deformed extrusive Eocene-Oligocene rocksalt from Eyvanekey plateau and Garmsar hills (central Iran). *Journal of Structural Geology*, **29**, 241-255. doi: 10.1016/j.jsg.2006.08.014

Schmid, S. M., Fügenschuh, B., Kissling, E. and Schuster, R., 2004. Tectonic map and overall architecture of the Alpine orogen. *Eclogae geologicae Helveticae*, **97**, 93–117. doi: 10.1007/s00015-004-1113-x

Schmid, S. M., Bernoulli, D., Fügenschuh, B., Matenco, L., Schefer, S., Schuster, R., Tischler, M. and Ustaszewski, K., 2008. The Alpine-Carpathian-Dinaridic orogenic system: Correlation and evolution of tectonic units. *Swiss Journal of Geosciences*, **101**, 139–183. http://dx.doi.org/10.1007/s00015-008-1247-3

Schorn, A. and Neubauer, F., 2011. Emplacement of an evaporitic mélange nappe in central Northern Calcareous Alps: evidence from the Moosegg klippe (Austria). *Austrian Journal of Earth Sciences*, **104**, 22-46.

Schorn, A., Neubauer, F., Genser, J., and Bernroider, M., 2013. The Haselgebirge evaporitic mélange in central Northern Calcareous Alps (Austria): Part of the Permian to Lower Triassic rift of the Meliata ocean? *Tectonophysics*, **583**, 28-48.

Strauss, P., Granado, P. and Muñoz, J.A., 2021. Subsidence analysis of salt tectonics-driven carbonate minibasins (Northern Calcareous Alps, Austria). *Basin Research*, **33**, 968-990. doi: 10.1111/bre.12500

Stüwe, K. and Schuster, R., 2010. Initiation of subduction in the Alps: Continent or ocean? *Geology*, **38**, 175-178. doi: 10.1130/G30528.1

Suzuki, H. and Gawlick, H.-J., 2009. Jurassic radiolarians from cherty limestones below the Hallstatt salt mine (Northern Calcareous Alps, Austria). *Neues Jahrbuch für Geologie und Palaontologie – Abhandlungen*, **251**, 155-197. doi: 10.1127/0077-7749/2009/0251-0155

Tollmann, A., 1987. Late Jurassic/Neocomian gravitational tectonics in the Northern Calcareous Alps in Austria. In: *Geodynamics of the Eastern Alps* (H.W. Flügel, P. Faupl, eds.), Franz Deuticke, 112-125.

Vozarova, A., Vozár, J. and Mayr, M., 1999. High-pressure metamorphism of basalts in the evaporite sequence of the Haselgebirge: An evidence from Bad Ischl (Austria). *Abhandlungen der geologischen Bundesanstalt*, **56**, 325-330.

Wagreich, M. and Decker, K., 2001. Sedimentary tectonics and subsidence modelling of the type Upper Cretaceous Gosau basin (Northern Calcareous Alps, Austria). *International Journal of Earth Sciences*, **90**, 714-726. doi: 10.1007/s005310000181

Wagreich, M. and Faupl, P. 1994. Palaeogeography and geodynamic evolution of the Gosau Group of the Northern Calcareous Alps (Late Cretaceous, Eastern Alps, Austria). *Palaeogeography, Palaeoclimatology, Palaeoecology*, **110**, 235-254. doi: 10.1016/0031-0182(94)90086-8

Závada, P., Bruthans, J., Adineh, S., Warsitzka, M. and Zare, M., 2021. Composition and deformation patterns of the caprock on salt extrusions in southern Iran – Field study on the Karmostaj and Siah Taq diapirs. *Journal of Structural Geology*, **151**, 104422. doi: 10.1016/j.jsg.2021.104422

Supplemental information 1: 3D outcrop of basal allochthon contact

The 3D model below has been generated from oblique photographs taken with a handheld digital Panasonic Lumix DMC-FZ1000 II camera with a 20 Megapixel CMOS-1" sensor. Images have been processed with a Structure from Motion algorithm (Agisoft Metashape Professional v. 1.8.3, www.agisoft.com) to generate a point cloud with 24,469,626 points and a textured mesh with 1,408,843 faces. The model has been georeferenced and scaled based on outcrop control points.

In the model the location of Fig. 3a and 3b are shown by the blue and dark orange spheres respectively (the blue sphere lies beyond the southern extent of the mesh). The yellow sphere indicates the location of the top of the Jurassic Ruhpolding Fm siliceous limestones and base of the allochthonous evaporite unit. The lowermost 3 meters of the evaporite unit are not directly visible and are covered by mud.

Supplemental information 2: 3D model of topography and dip data

The 3D model of the Wurzeralm study area includes the downsampled topography (Geoland.at, 2015) draped with the geological map of Figure 1a and a selection of dip measurements manually filtered for representativity, to avoid clutter. Dip data (represented by orientated disks) are derived from either bedding dip measurements acquired by the co-authors in the field or from analysis of digital topography and 3D digital outcrop data, following the approach described in Fernandez et al. (2009).

Note that the basal contact of the Wurzeralm allochthonous salt body can be traced around the outcrop of the allochthon, with dips of the underlying Ruhpolding Fm indicating this unit dips under the allochthonous Haselgebirge and Werfen Fms. Furthermore, the basal contact of the allochthon strikes roughly parallel to the stratigraphic contact between the Ruhpolding Fm and the underlying Klaus Fm or Dachstein Limestone, indicating the contact has a similar dip and trend (i.e., roughly parallel to bedding).

Supplemental information 3: Folding in the Ruhpolding Fm

Folding in the Ruhpolding Fm is found to follow two main trends roughly perpendicular to each other: NE-SW and NW-SE.

SI.3a: Location of selected detailed observations of deformation involving the Ruhploding Fm in the study area. This map and its color legend are equivalent to those in Figure 1c.

SI.3b: Outcrop view (from UTM33 446210E 5276624N) trending roughly E-W (slope trends NE-SW) of an imbricate thrust system causing a repetition of the Oberalm, Ruhpolding and Haselgebirge Fms. The structures trend roughly NW-SE. Note that the stretching lineation is parallel to the trend of the folds and faults in the Jurassic units, with a broad scatter of foliation planes in the Haselgebirge Fm, raising the possibility that the fabric is nearly a purely constrictional fabric associated to folding-thrusting (cf. Fig. 8, Sullivan, 2013). Thrusting and

folding are considered to be posterior to Ruhpolding Fm consolidation, as they involve the entire Oberalm Fm as well. The origin is therfore either tectonic or related to salt-sheet emplacement.

SI.3c,d: Drone-acquired aerial oblique views of an outcrop (UTM33 446105E 5276624N) exhibiting complex folding within the Ruhpolding Fm. A common point on both photos is indicated by a black line joining them. Fold axes (measured, as well as best-fit calculations) have a NE-SW trend. The outcrop exhibits a chaotic structure in its eastern segment (SI.3d) and partially distorted beds in the western segment, recognized by the more nodular geometry in the core of the main fold structure (SI.3c). This is interpreted to result from syn-sedimentary to shallow-burial deformation. The main fold structure of the western segment (SI.3c) shows constant-thickness bedding and geometries reminiscent of post-burial (consolidated) state deformation (M crestal fold). However, given the limited amount of maximum burial of the area (e.g., Kralik et al., 1987; Gawlick et al., 1994), the tightness of folding is easier to explain assuming the radiolarite unit was not fully consolidated. The dimensions of these folds (tens of meters) are compatible to those of other known soft-sediment deformation folds (e.g., Ortner, 2007).

SI.3e: Outcrop view (UTM33 446115E 5276815N) trending roughly N-S of Ruhpolding Fm beds affected by folding with NW-SE trending fold axes that overprint initial folding and truncation of beds related to syn-sedimentary deformation. In this outcrop two fold axes have been estimated. One fold axis has been estimated from beds that have been steepened by the NW-SE trending fold and coincides with a minor fold axis measured in the field (outside the field of the photo). The second fold axis has been determined for beds that appear truncated (as these clearly relate to syn-sedimentary deformation). Although the best-fit calculation in this case is based on little data, it indicates in any case a fold axis that trends at a significantly high angle to the first axis, and that plunges roughly parallel to bedding (as would be expected for a syn-sedimentary fold).

References

Fernandez, O., Jones, S., Armstrong, N., Johnson, G., Ravaglia, A., Muñoz, J.A., 2009. Automated tools within workflows for 3D structural construction from surface and subsurface data. *Geoinformatica*, **13**, 291-304. doi: 10.1007/s10707-008-0059-y

Gawlick, H.-J., Krystyn, L., Lein, R., 1994. Conodont colour alteration indices: Palaeotemperatures and metamorphism in the Northern Calcareous Alps - a general view. *Geologische Rundschau*, **83**, 660-664.

Geoland.at, 2015. Digital terrain model of Austria, based on airborne laserscanning. Geoland.at. https://www.data.gv.at/katalog/de/dataset/dgm

Kralik, M., Krumm, H., Schramm, J.M., 1987. Low grade and very low grade metamorphism in the Northern Alps and in the Grauwacke Zone: Illite-crystallinity data and isotopic ages. In: *Geodynamics of the Eastern Alps* (H.W. Flügel, P. Faupl, eds.), Franz Deuticke, 164-178.

Ortner, H., 2007. Styles of soft-sediment deformation on top of a growing fold system in the Gosau Group at Muttekopf, Northern Calcareous Alps, Austria: Slumping versus tectonic deformation. *Sedimentary Geology*, **196**, 99-118. doi: 10.1016/j.sedgeo.2006.05.028

Sullivan, W.A., 2013. L tectonites. *Journal of Structural Geology*, **50**, 161-175.

Sl.1. 3D outcrop of basal allochthon contact

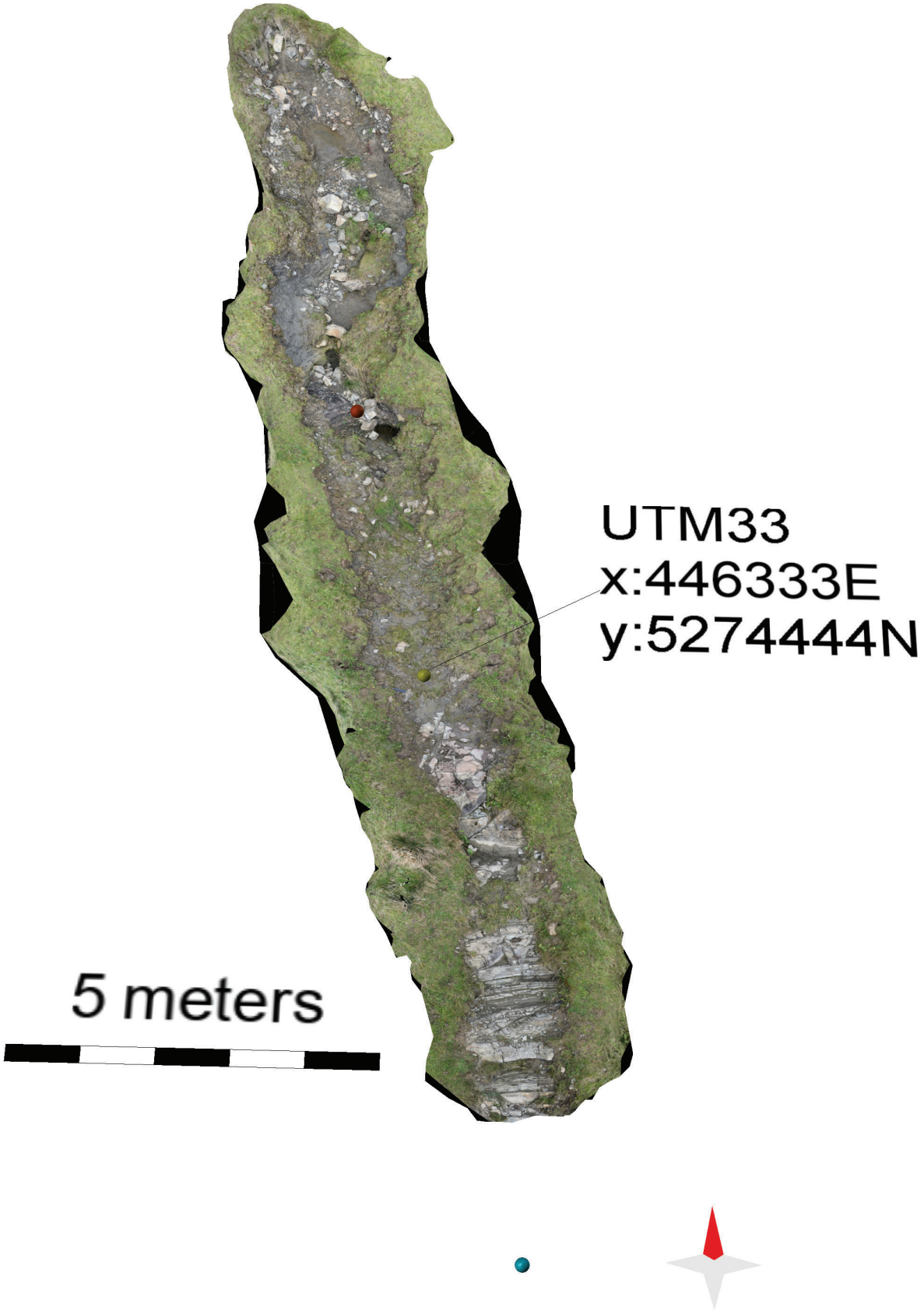

SI.2. 3D model of topography and dip data

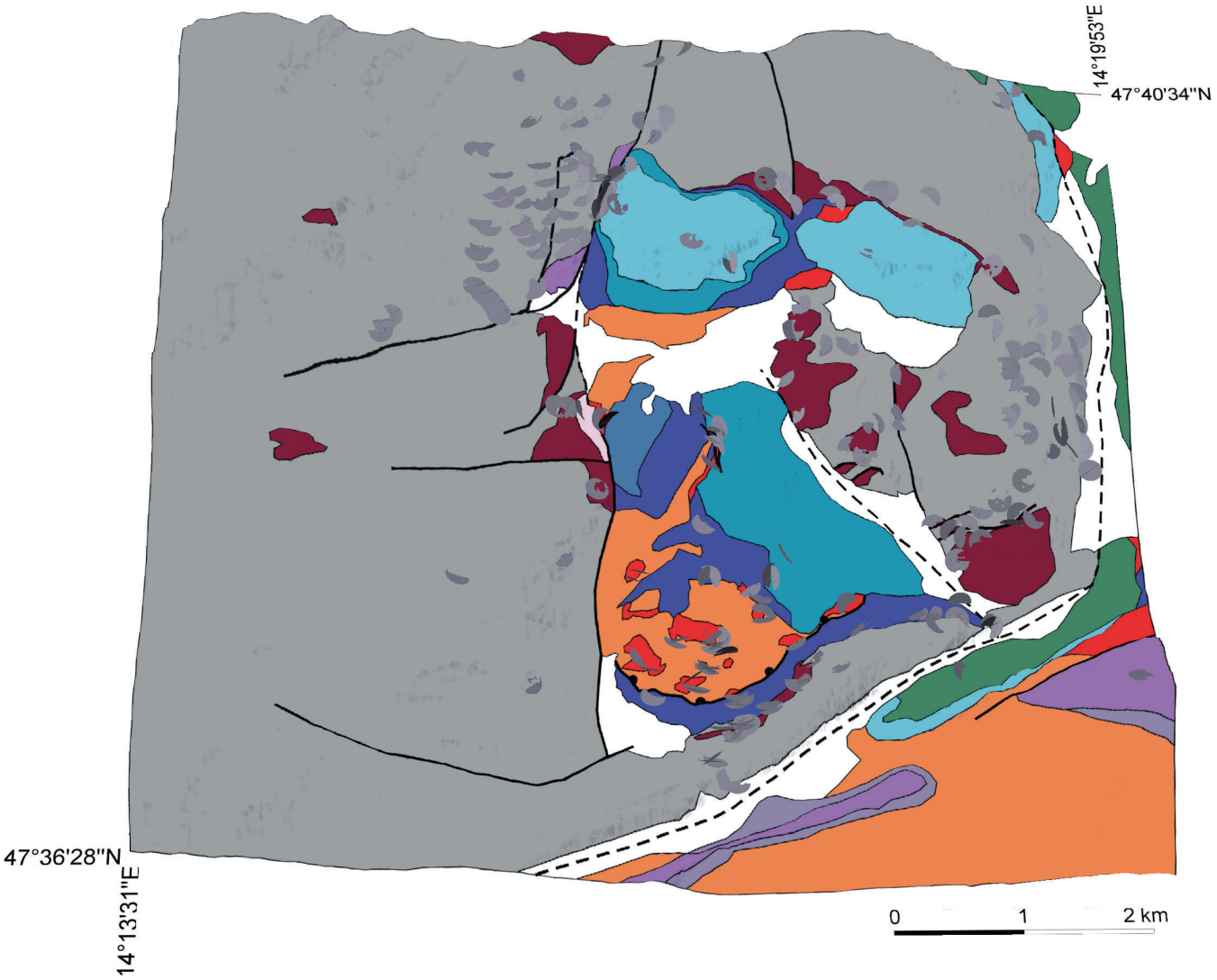

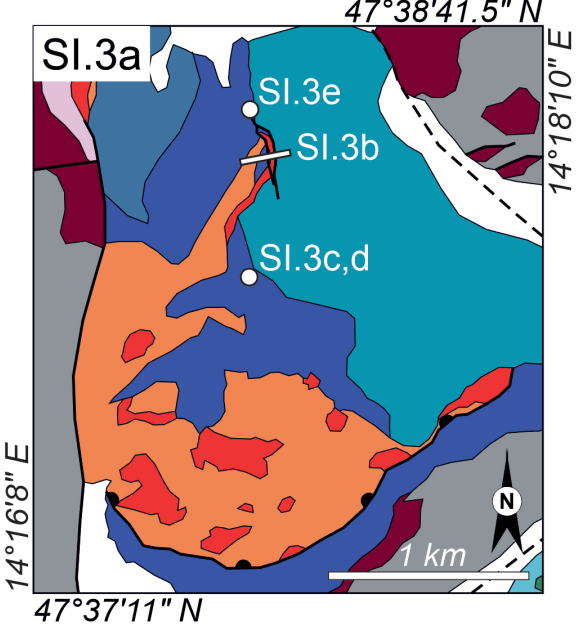

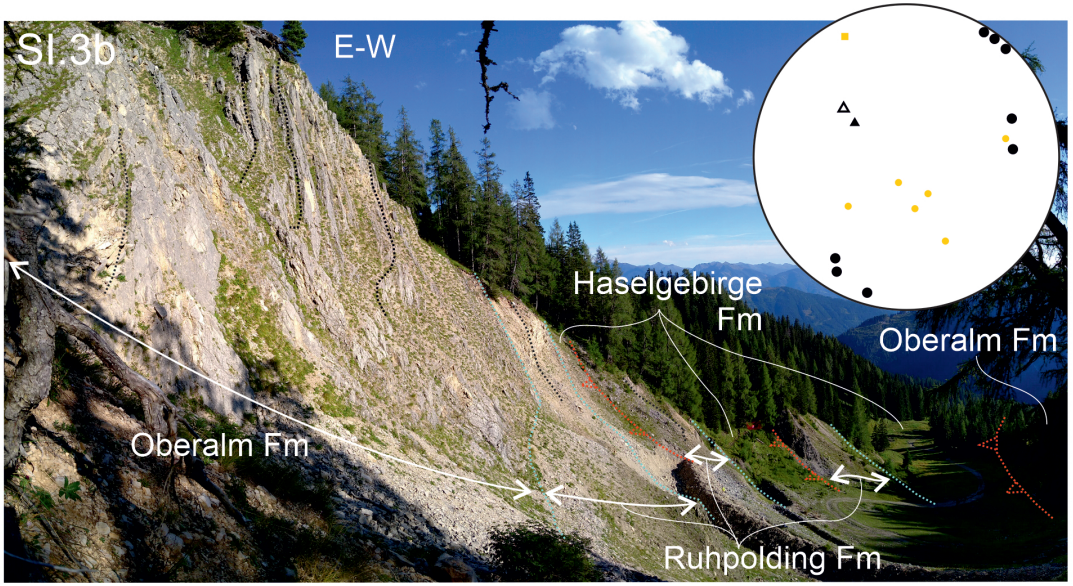

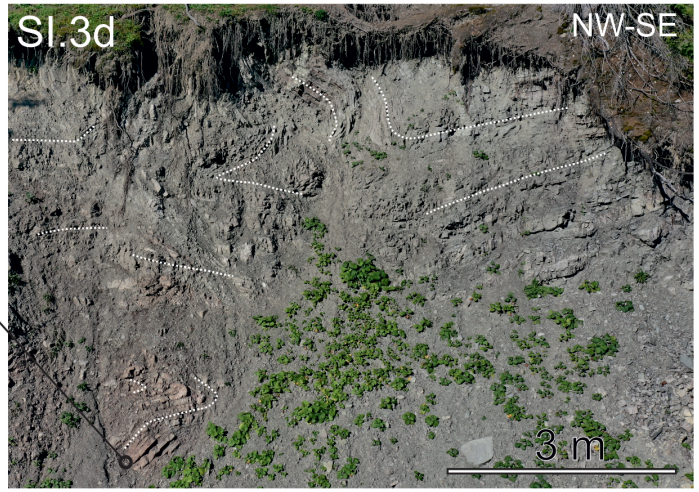

Photo-interpretation

- bedding
- truncated bedding
- stratigraphic contact
- thrust

Stereoplots

NE-SW trend	NW-SE trend	
	●	bedding
▲	▲	measured fold axis
△	△	best-fit fold axis
		Haselgebirge Fm: stretching lineation
		Haselgebirge Fm: foliation